Original Article

Ternary hybrid nanocomposites for gene delivery and magnetic resonance imaging of hepatocellular carcinoma cells

Ken Cham-Fai Leung[1], Chi-Hin Wong[1], Xiao-Ming Zhu[1,2], Siu-Fung Lee[3], Kathy W. Y. Sham[4], Josie M. Y. Lai[4], Chun-Pong Chak[3], Yi-Xiang J. Wang[2], Christopher H. K. Cheng[4]

[1]Department of Chemistry and Institute of Creativity, The Hong Kong Baptist University, Kowloon Tong, Kowloon, Hong Kong SAR, P. R. China; [2]Department of Imaging and Interventional Radiology, Prince of Wales Hospital, [3]Department of Chemistry, [4]School of Biomedical Sciences, The Chinese University of Hong Kong, Shatin, NT, Hong Kong SAR, P. R. China

Corresponding to: Ken Cham-Fai Leung. Department of Chemistry and Institute of Creativity, The Hong Kong Baptist University, Kowloon Tong, Kowloon, Hong Kong SAR, P. R. China. Email: cfleung@hkbu.edu.hk; Yi-Xiang J. Wang. Department of Imaging and Interventional Radiology, Prince of Wales Hospital, The Chinese University of Hong Kong, Shatin, NT, Hong Kong SAR, P. R. China. Email: yixiang_wang@cuhk.edu.hk; Christopher H. K. Cheng. School of Biomedical Sciences, The Chinese University of Hong Kong, Shatin, NT, Hong Kong SAR, P. R. China. Email: chkcheng@cuhk.edu.hk.

Abstract: This paper describes comparative studies in magnetic resonance imaging (MRI) and gene deliveries toward hepatocellular carcinoma (HCC) HepG2 cells with ternary composites that consist of superparamagnetic iron oxide (SPIO) nanoparticles (NPs) (8-10 nm) with deferoxamine coating, circular plasmid DNA (~4 kb) equipped with green fluorescent probe, and branched polyethylenimine (PEI) (25 kDa, PDI 2.5). The packaging of the ternary complexes has been characterized by agarose gel retardation assay. By tuning the PEI/NP ratios and with a fixed DNA amount, different ternary composites have been employed for NP/gene transfection towards HepG2 cells, which have been characterized by *in vitro* MRI and green fluorescence protein (GFP) fluorescence.

Keywords: Deferoxamine; gene delivery; hepatocellular carcinoma (HCC); magnetic resonance imaging (MRI); superparamagnetic iron oxide (SPIO)

Submitted Nov 28, 2013. Accepted for publication Dec 13, 2013.
doi: 10.3978/j.issn.2223-4292.2013.12.05
Scan to your mobile device or view this article at: http://www.amepc.org/qims/article/view/3108/3995

The development of diagnostic and therapeutic nanomaterials (1-8) for drug/gene co-delivery and ultrasonic/magnetic resonance imaging (MRI) contrast enhancement has been progressing rapidly towards various cancer cell types, especially in brain (9), liver (10-13), and other sites (14-22). In particular, ultrasmall superparamagnetic iron oxide (SPIO) nanoparticles (NPs) offer cell tracking, targeting, and substrate delivery to specific target site(s) (23-25). Linear polyethylenimine (PEI) polymers of low or high molecular weights have been employed to deliver genes with enhanced transfection efficiencies and possibly reducing cytotoxicities (26,27). In particular, ultrasmall deferoxamine-coated SPIO-NPs were first reported in our group (9,12) and studied for their biomedical properties. Deferoxamine, also known as desferal, is a clinically approved drug to treat iron poisoning. Slow degradation of iron oxide NPs *in vivo* will result in soluble iron ions which will, in turn, capture by deferoxamine layer at the nanoparticle's periphery. Eventually, the deferoxamine-iron complexes will be excreted in the urine, thus reducing the *in vivo* toxicity especially in the heart and liver.

In view of delivering genes and facilitating MRI towards hepatocellular carcinoma (HCC) HepG2 cells with enhanced cellular uptake or transfection efficiencies, we report herein the use of deferoxamine-coated ultrasmall (8-10 nm) Fe_3O_4 SPIO-NPs (23-25), hybridizing with circular plasmid DNAs (pEGFP-C1), and branched PEI (25 kDa, PDI =2.5) to furnish ternary composites (9,12,13,26-32) for MRI and fluorescence imaging. The

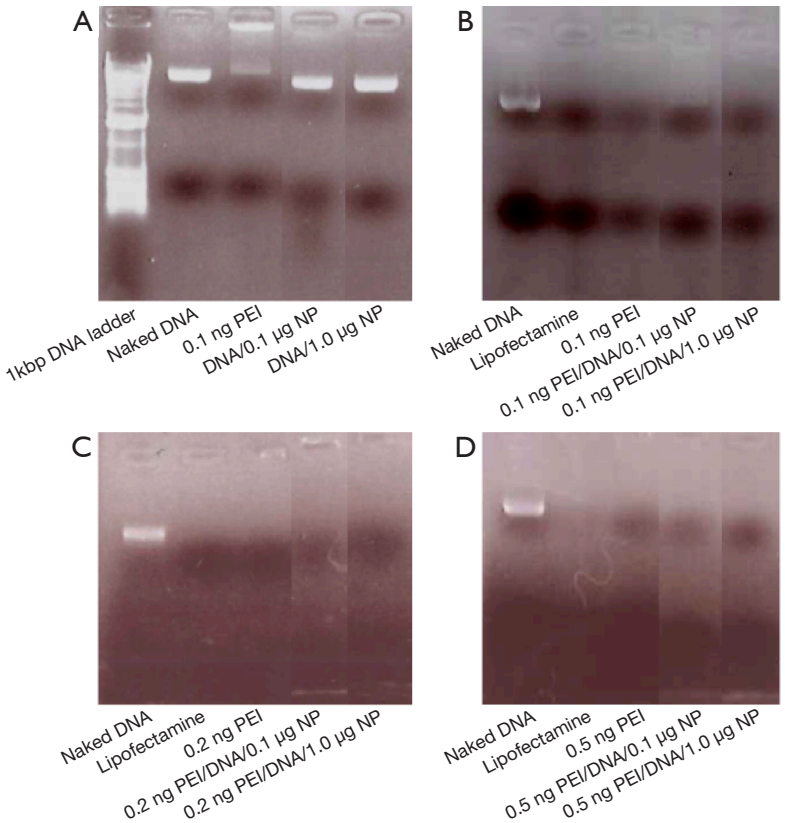

Figure 1 Gel electrophoresis on 1% agarose gel whereas the DNA (pEGFP-C1) concentration is fixed at 0.5 μg/well.

biocompatibility of the ternary complex was evaluated by agarose gel retardation assay. The cellular uptake of the ternary complex is proposed by the receptor-mediate endocytosis (13,33,34) of HCC cells. Circular plasmid DNA pEGFP-C1 (~4.7 kb, Clontech) encodes a red-shifted variant of wild-type green fluorescence protein (GFP) in mammalian cells. The plasmid was prepared by using the QIAprep Spin Miniprep Kit (QIAGEN) with A_{260}/A_{280} ratio larger than 1.8. The fluorescence intensity is directly proportional to the amount of GFP expressed in the cells. By the strong, enhanced and constitutive expression of the reporters, the signals can be easily detected. They are optimized so that the reporters can be expressed in a variety of cell types/lines. It is envisaged that after receptor-mediated endocytosis of the composites, the NPs in the composites would be cleaved and localized in the cytoplasm, which is responsible for generating MRI dark contrast signal. On the other hand, the pDNA of the composites would be further imported into the nucleus, which is responsible for expressing the fluorescence.

NPs with a deferoxamine coating could be self-assembled with negatively charged pDNA and positively charged branched PEI to furnish the ternary composites (200-300 nm) (9,12,13), thereby stabilizing by multiple electrostatic interaction and hydrogen bonds (35,36). The morphology and surface functional groups of the composites were characterized by transmission electron microscopy (TEM) and Infrared (IR) absorption spectroscopy, respectively, which were reported previously in the literature. To evaluate the pDNA condensation ability of the PEI, agarose gel retardation assay was performed. The samples were then loaded onto 1% agarose gel containing 1× RedSafe Nucleic Acid staining solution (iNtRon Biotechnology). Free DNA (naked DNA) and commercially available transfecting agent Lipofectamine (Life Technologies) were used as controls. After electrophoresis (*Figure 1*) carried out at 110 V in tris-acetate-EDTA buffer (pH 7.4), uncomplexed (free) pDNA will migrate into the gel. RedSafe staining dye will stain the pDNA and DNA bands can then be visualized under a UV transilluminator. On the other hand, PEI and PEI/NP can retard the pDNA migration toward the cathode

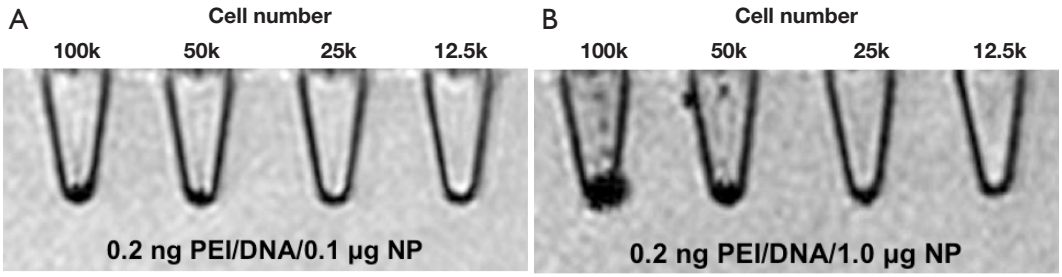

Figure 2 Gradient echo *in vitro* MRI images of composite-transfected HepG2 cells in Eppendorf tubes with culture medium. The amount of DNA (pEGFP-C1) of both complexes is fixed at 0.5 μg/well.

and exclude the dye from staining the nucleic acid. By observing the presence or absence of band and band intensity with the use of NPs, the pDNA packaging can be monitored, which is a critical step before transfection by the assay.

HCC HepG2 cells (ATCC, Manassas, VA) were cultured with DMEM (Life Technologies) containing 10% fetal bovine serum (FBS), 100 U/mL penicillin, and 100 μg/mL streptomycin at 37 ℃ and in a humidified 5% CO_2 atmosphere. Subsequently, about 50,000 cells were seeded onto each well of the 24- or 96-well plates. After 24 h, the culture medium was replaced with the serum-free DMEM containing different composites. After incubation for 5 h, the medium was aspirated and refreshed with complete DMEM. The cells were further incubated for 24 h at 37 ℃. Colorimetric method was used to study the iron concentration for the cells that were transfected with the composites. The cells were washed, collected, and counted for the intracellular iron content quantification. After centrifugation (4,500 g) for 5 min, the collected cell pellets were dispensed in 100 μL 12% HCl solution and incubated at 60 ℃ for 4 h. After incubation, the suspension was centrifuged (12,000 g) for 10 min, whereas the supernatants were collected for iron concentration quantification. A sample solution (50 μL) was added into the wells of a 96-well plate, and then ammonium persulfate (50 μL, 1%) was added to oxidize the ferrous ions into ferric ions. Finally, potassium thiocyanate (100 μL, 0.1 M) was added to the solution and incubated for 5 min to form the red color of iron-thiocyanate. The absorption at 490 nm of the sample was observed on a microplate reader (Bio-Rad, Model 3550).

In vitro MRI was performed with HepG2 cells 24 h after transfection. After washing with PBS, the cells were trypsinized and counted. Different numbers (12.5, 25, 50, and 100 k) of cells were placed in an Eppendorf tube (1.5 mL) separately. After a centrifugation at 3,000 g for 5 min, the Eppendorf tubes were placed perpendicular to the main magnetic induction field (B_0) in a 20 cm × 12 cm × 8 cm water bath. MRI was performed with a 3.0-T clinical whole-body magnetic resonance unit (Achieva, Philips Medical Systems), using a transmit-receive head coil. T_2 relaxation times were measured by using a standard Carr–Purcell–Meiboom–Gill pulse sequence [repetition time (TR) =2,000 ms, echo time (TE) range =30-960 ms, 32 echoes, field-of-view (FOV) =134×67 mm^2, matrix =128×64, slice thickness =5 mm, number of excitations =3]. The magnetic resonance sequence was a two-dimensional gradient-echo sequence with TR/TE =400/48 ms, flip angle =18°, matrix =512×256, resolution =0.45×0.45 mm, slice thickness =2 mm, and number of excitations =2. Sagittal images were obtained through the central section of the bottom tips of the Eppendorf tubes. HepG2 cells were transfected separately with ternary complexes of varying NP concentrations and analyzed by *in vitro* MRI. Substantial negative (dark) contrast MRI signals with "ballooning" effect are observed in *Figure 2* with the cells that were centrifugated at the bottom of Eppendorf tube. Under fixed amounts of PEI (0.2 ng) and DNA (0.5 μg) per well, HepG2 cells that were transfected with higher NP concentrations possessed stronger MRI dark contrast signals. For ternary complexes containing 0.1 and 1.0 μg NP, MRI signals were detectable and visually observable at cell number of 100, 50, 25, and 12.5 k, respectively. T_2 relaxation times were calculated by fitting the logarithmic region of interest signal amplitudes (1,600 pixel) versus TE. The T_2 relaxivities (r_2) were determined by a linear fit of the inverse relaxation times as a function of the iron concentrations used. The *in vitro* r_2 of the two composites 0.2 ng PEI/0.5 μg DNA/0.1 μg NP and 0.2 ng PEI/0.5 μg DNA/1.0 μg NP were determined to be 1.46 and 2.20 s^{-1} mM^{-1} Fe, respectively. Prussian blue staining

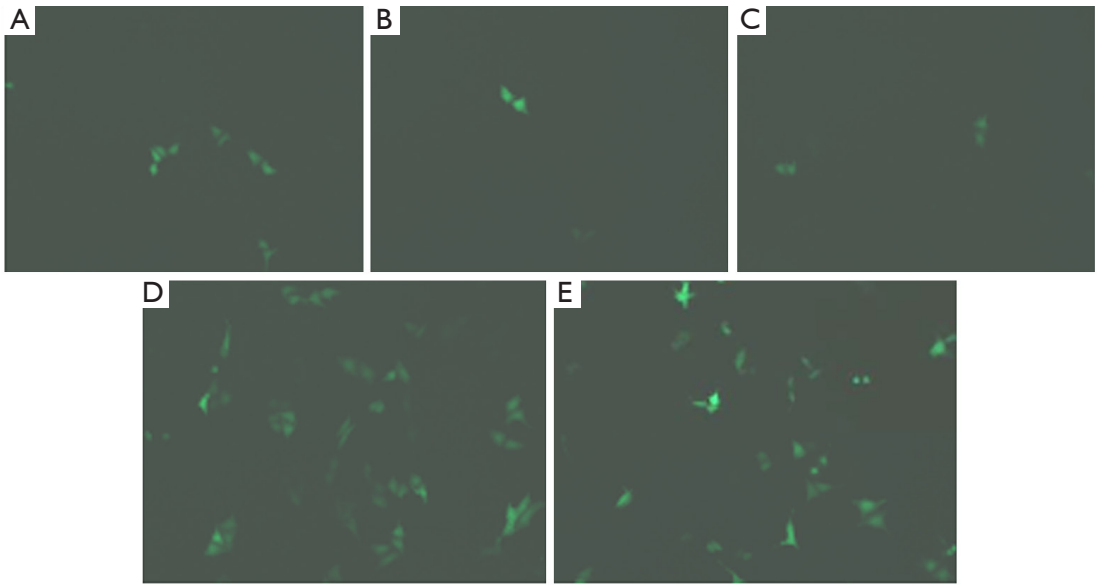

Figure 3 GFP fluorescence images of HepG2 cells separately transfected after 5 h with (A-C) different ternary composites 0.1 ng PEI/0.5 μg DNA/NP with varying amounts of NP (A, 0.1 μg, B, 1.0 μg, and C, 2.5 μg), (D) 0.1 ng PEI/0.5 μg DNA, and (E) Lipofectamine/0.5 μg DNA.

(9,12,17-19,23-25) is an alternative method to quantify the *in vitro* iron content. These results suggest that the ternary hybrid nanocomposites hold promise as effective MRI contrast agents and are potentially suitable for magnetic targeting to cancer sites.

About 50,000 cells were seeded onto each well of the 24-well plates for GFP observation. The typical GFP green fluorescent images of HepG2 cells which have been separately transfected with (A-C) different ternary composites 0.1 ng PEI/0.5 μg DNA/NP with varying amounts of NP (A: 0.1 μg, B: 1.0 μg, and C: 2.5 μg), (D) 0.1 ng PEI/0.5 μg DNA, and (E) Lipofectamine/0.5 μg DNA, are shown in *Figure 3*. The green fluorescence of the transfected HepG2 cells was visualized by a Nikon TE2000 fluorescence microscope 24 h after transfection. According to the visual assessment of these images, the cellular uptake efficiencies of the pDNA in the ternary complexes (*Figure 3A-C*) to the HepG2 cell nucleus generally lower than that using Lipofectamine or PEI (*Figure 3C,D*). However, the cellular uptake efficiencies of the pDNA in the ternary complexes (*Figure 3A-C*) to the HepG2 cell nucleus will be greatly enhanced 24 h after transfection (12). It is reasonably to consider that the cellular uptake efficiency depends on the surface charge density and stability of the composites during the receptor-mediated endocytosis and further cleavage of the composite with NP localized in cytoplasm and pDNA in nucleus. The transfected composites would eventually be dissociated into separate components and subject to an efflux mechanism. Moreover, cytotoxicities of cells incubated with the composites in working concentrations that were examined by methylthiazolyldiphenyl-tetrazolium (MTT) bromide assay in HepG2 cells, have been reported. The cell viabilities range from 70% to 85%, which are higher than using Lipofectamine or PEI (12).

In conclusion, ternary composites based on PEI/DNA/deferoxamine-NP have been prepared by tuning the PEI/NP ratios and with a fixed DNA amount, for transfection towards HCC HepG2 cells. The cell transfection efficiencies involving NP uptake and gene expression with the ternary composites could be altered by tuning the PEI/NP ratios in the composite, which have been characterized by *in vitro* MRI and GFP fluorescence. From the MRI assessments, the *in vitro* r_2 values of ternary complexes 0.2 ng PEI/0.5 μg DNA/0.1 μg NP and 0.2 ng PEI/0.5 μg DNA/1.0 μg NP were determined to be 1.46 and 2.20 s^{-1} mM^{-1} Fe, respectively. The as-prepared composites or other nanostructured magnetic composites (37) offer potential biomedical applications in simultaneous gene delivery, imaging contrast enhancement, and metabolism study for the next generation *in vivo* carcinoma nano-theranostic purpose.

Acknowledgements

We acknowledge the financial support by a General Research Fund (201213) from The Hong Kong Research Grants Council.

This study is also partially supported by the direct grant for research by the Chinese University of Hong Kong (No.4054012).

Disclosure: The authors declare no conflict of interest.

References

1. Moyano DF, Rotello VM. Nano meets biology: structure and function at the nanoparticle interface. Langmuir 2011;27:10376-85.
2. Chen X, Gambhir SS, Cheon J. Theranostic nanomedicine. Acc Chem Res 2011;44:841.
3. Kharissova OV, Kharisov BI, Jiménez-Pérez VM, et al. Ultrasmall particles and nanocomposites: state of the art. RSC Adv 2013;3:22648-82.
4. Li L, Jiang W, Luo K, et al. Superparamagnetic iron oxide nanoparticles as MRI contrast agents for non-invasive stem cell labeling and tracking. Theranostics 2013;3:595-615.
5. Kelkar SS, Reineke TM. Theranostics: combining imaging and therapy. Bioconjug Chem 2011;22:1879-903.
6. Algar WR, Prasuhn DE, Stewart MH, et al. The controlled display of biomolecules on nanoparticles: a challenge suited to bioorthogonal chemistry. Bioconjug Chem 2011;22:825-58.
7. Smith BA, Smith BD. Biomarkers and molecular probes for cell death imaging and targeted therapeutics. Bioconjug Chem 2012;23:1989-2006.
8. Xuan S, Wang F, Gong X, et al. Hierarchical core/shell Fe3O4@SiO2@γ-AlOOH@Au micro/nanoflowers for protein immobilization. Chem Commun (Camb) 2011;47:2514-6.
9. Leung KC, Chak CP, Lee SF, et al. Enhanced cellular uptake and gene delivery of glioblastoma with deferoxamine-coated nanoparticle/plasmid DNA/branched polyethylenimine composites. Chem Commun (Camb) 2013;49:549-51.
10. Lu J, Ma S, Sun J, et al. Manganese ferrite nanoparticle micellar nanocomposites as MRI contrast agent for liver imaging. Biomaterials 2009;30:2919-28.
11. Tam KY, Leung KC, Wang YX. Chemoembolization agents for cancer treatment. Eur J Pharm Sci 2011;44:1-10.
12. Leung KC, Chak CP, Lee SF, et al. Increased efficacies in magnetofection and gene delivery to hepatocellular carcinoma cells with ternary organic-inorganic hybrid nanocomposites. Chem Asian J 2013;8:1760-4.
13. Leung KC, Lee SF, Wong CH, et al. Nanoparticle-DNA-polymer composites for hepatocellular carcinoma cell labeling, sensing, and magnetic resonance imaging. Methods 2013;64:315-21.
14. Chou LY, Ming K, Chan WC. Strategies for the intracellular delivery of nanoparticles. Chem Soc Rev 2011;40:233-45.
15. Xuan S, Wang F, Lai JM, et al. Synthesis of biocompatible, mesoporous Fe(3)O(4) nano/microspheres with large surface area for magnetic resonance imaging and therapeutic applications. ACS Appl Mater Interfaces 2011;3:237-44.
16. Leung KC, Xuan S, Zhu X, et al. Gold and iron oxide hybrid nanocomposite materials. Chem Soc Rev 2012;41:1911-28.
17. Zhu XM, Yuan J, Leung KC, et al. Hollow superparamagnetic iron oxide nanoshells as a hydrophobic anticancer drug carrier: intracelluar pH-dependent drug release and enhanced cytotoxicity. Nanoscale 2012;4:5744-54.
18. Xuan SH, Lee SF, Lau JT, et al. Photocytotoxicity and magnetic relaxivity responses of dual-porous γ-Fe2O3@meso-SiO2 microspheres. ACS Appl Mater Interfaces 2012;4:2033-40.
19. Lee SF, Zhu XM, Wang YX, et al. Ultrasound, pH, and magnetically responsive crown-ether-coated core/shell nanoparticles as drug encapsulation and release systems. ACS Appl Mater Interfaces 2013;5:1566-74.
20. Wang DW, Zhu XM, Lee SF, et al. Folate-conjugated Fe3O4@SiO2@gold nanorods@mesoporous SiO2 hybrid nanomaterial: a theranostic agent for magnetic resonance imaging and photothermal therapy. J Mater Chem B 2013;1:2889-93.
21. Wang YX, Wang DW, Zhu XM, et al. Carbon coated superparamagnetic iron oxide nanoparticles for sentinel lymph nodes mapping. Quant Imaging Med Surg 2012;2:53-6.
22. Lee JH, Chen KJ, Noh SH, et al. On-demand drug release system for in vivo cancer treatment through self-assembled magnetic nanoparticles. Angew Chem Int Ed Engl 2013;52:4384-8.
23. Wang HH, Wang YX, Leung KC, et al. Durable mesenchymal stem cell labelling by using polyhedral superparamagnetic iron oxide nanoparticles. Chemistry 2009;15:12417-25.

24. Wang YX, Quercy-Jouvet T, Wang HH, et al. Efficacy and durability in direct labeling of mesenchymal stem cells using ultrasmall superparamagnetic iron oxide nanoparticles with organosilica, dextran, and PEG coatings. Materials 2011;4:703-15.
25. Zhu XM, Wang YX, Leung KC, et al. Enhanced cellular uptake of aminosilane-coated superparamagnetic iron oxide nanoparticles in mammalian cell lines. Int J Nanomedicine 2012;7:953-64.
26. Lee Y, Miyata K, Oba M, et al. Charge-conversion ternary polyplex with endosome disruption moiety: a technique for efficient and safe gene delivery. Angew Chem Int Ed Engl 2008;47:5163-6.
27. Wang XL, Zhou LZ, Ma YJ, et al. Charged magnetic nanoparticles for enhanced gene transfection. IEEE Trans Nanotechnol 2009;8:142-7.
28. Miyata K, Gouda N, Takemoto H, et al. Enhanced transfection with silica-coated polyplexes loading plasmid DNA. Biomaterials 2010;31:4764-70.
29. Cabral H, Kataoka K. Multifunctional nanoassemblies of block copolymers for future cancer therapy. Sci Technol Adv Mater 2010;11:014109.
30. Liu WM, Xue YN, Peng N, et al. Dendrimer modified magnetic iron oxide nanoparticle/DNA/PEI ternary magnetoplexes: a novel strategy for magnetofection. J Mater Chem 2011;21:13306-15.
31. Vachutinsky Y, Oba M, Miyata K, et al. Antiangiogenic gene therapy of experimental pancreatic tumor by sFlt-1 plasmid DNA carried by RGD-modified crosslinked polyplex micelles. J Control Release 2011;149:51-7.
32. Chen K, Xie J, Xu H, et al. Triblock copolymer coated iron oxide nanoparticle conjugate for tumor integrin targeting. Biomaterials 2009;30:6912-9.
33. Mu Q, Hondow NS, Krzemiński L, et al. Mechanism of cellular uptake of genotoxic silica nanoparticles. Part Fibre Toxicol 2012;9:29.
34. He X, Nie H, Wang K, et al. In vivo study of biodistribution and urinary excretion of surface-modified silica nanoparticles. Anal Chem 2008;80:9597-603.
35. South CR, Leung KCF, Lanari D, et al. Noncovalent side-chain functionalization of terpolymers. Macromolecules 2006;39:3738-44.
36. Chak CP, Xuan S, Mendes PM, et al. Discrete functional gold nanoparticles: hydrogen bond-assisted synthesis, magnetic purification, supramolecular dimer and trimer formation. ACS Nano 2009;3:2129-38.
37. Leung KC, Wang YX, Wang H, et al. Biological and magnetic contrast evaluation of shape-selective Mn-Fe nanowires. IEEE Trans Nanobioscience 2009;8:192-8.

Cite this article as: Leung KCF, Wong CH, Zhu XM, Lee SF, Sham KWY, Lai JMY, Chak CP, Wang YXJ, Cheng CHK. Ternary hybrid nanocomposites for gene delivery and magnetic resonance imaging of hepatocellular carcinoma cells. Quant Imaging Med Surg 2013;3(6):302-307. doi: 10.3978/j.issn.2223-4292.2013.12.05

